44th AIAA/ASME/ASCE/AHS Structures, Structural Dynamics, and Materials Confere
7-10 April 2003, Norfolk, Virginia

AIAA 2003-1411

HYBRID FREQUENCY-TIME DOMAIN METHODS FOR THE ANALYSIS OF COMPLEX STRUCTURAL SYSTEMS WITH DRY FRICTION DAMPING

Olivier Poudou
Graduate Student
Department of Mechanical Engineering
University of Michigan
2277 G.G. Brown Building,
Ann Arbor, MI-48109-2125, USA
Email: poudou@umich.edu

Christophe Pierre*
Professor, Senior Member of AIAA
Department of Mechanical Engineering
University of Michigan
3112 G.G. Brown Building
Ann Arbor, MI-48109-2125, USA
Email: pierre@umich.edu

**Address correspondence to this author*

ABSTRACT

This paper considers the dynamics of complex structures with dry friction dampers attached, such as turbomachinery bladed disks. Two extensions of the Hybrid Frequency/Time domain (HFT) method are introduced to calculate efficiently the steady-state forced response of (1) realistic, tuned assemblies with cyclic properties; and (2), structures represented by reduced-order models which feature - for sake of accuracy and convenience – a high ratio of linear degrees of freedom to nonlinear frictional degrees of freedom. It is shown in particular that for cyclic systems, considering the disk as a rigid support is no longer required to carry out the nonlinear analysis, and that the exact dynamics of a flexible bladed-disk structure can be entirely deduced from the dynamics of one of its sectors. Three numerical examples are also presented. They show that the proposed modifications of the HFT method allow one to study with great efficiency the dynamics of complex, tuned or mistuned flexible assemblies, without sacrificing (1) the fidelity of the modeling of the structure, (2) the realism of the modeling of the frictional interfaces, which can possibly involve variable normal load and lost of contact; and (3), the accuracy of the nonlinear analysis, that is, the number of Fourier coefficients retained to approximate the periodic, steady-state response of the structure.

1. INTRODUCTION

Many studies on the dynamics of periodically excited structural systems with friction damping use the Harmonic Balance Method (HBM).[1] This method is based on the representation of the dynamics of the structure using a linear combination of temporal harmonics, and it is particularly well suited to the analysis of the steady state response of nonlinear systems. If a sufficient number of harmonics are retained, both the motion of selected degrees of freedom of the structure and the friction force at the contact points can be approximated with excellent accuracy.

Early studies on the subject of dry-friction damping were limited to single harmonic approximations. Among them, cantilevered beams[2–5] and simple turbomachinery applications[6–9] were successfully studied with models of dampers of increasing complexity, such as models with microslip,[10] variable normal load,[11] elliptic motion of the contact point,[12–14] or three dimensional contact kinematics.[15] However, it was also noted that the single harmonic approximation was often unable to accurately capture the periodic waveforms of the nonlinear response and the friction force.

This issue was first addressed by the introduction of an incremental variant of the HBM,[16,17] but the first multiharmonic studies[18] still required complicated analytical work to calculate the nonlinear force.

A significant breakthrough was made as the Alternating Frequency/Time domain method was introduced in 1989 by Cameron and Griffin.[19] It was realized that the nonlinearities due to the friction force can be accurately evaluated in the time domain and transformed back in the frequency domain, so as to form a set of nonlinear equations which can be solved by a Newton-Raphson-like procedure. Guillen and Pierre[20] recently proposed a variant of the AFT method, called Hybrid Frequency/Time

domain method, and confirmed that large scale, friction-damped systems can be efficiently studied with this approach.

Finally, the most recent works show that the HFT method is adapted to the study of systems featuring complex frictional nonlinearities with an accurate, multi-harmonic approach. Guillen *et al.*[21] introduced a flexible, structure-like damper model. Chen and Menq[22] developed a three-dimensional model of shroud contact, and, Nacivet *et al.*[23,24] introduced an alternative to the HFT method based on dynamic lagrangians.

This paper presents two extensions of the Hybrid Frequency/Time domain method:

The first one is based on Lagrange's work on the modeling of the forced response of spatially cyclic structures with friction dampers.[25] Previous works on this subject always assumes that the sectors of the assembly are structurally independent, that is, they are represented by independent structures connected to a rigid support. Coupling between these structures was assumed to occur only through the nonlinear forces, which depend from the motion of two adjacent sectors, such as the forces created by shroud-to-shroud contact or by underplatform dampers. In other words, these studies considered that for a bladed-disk assembly subject to nonlinear forces applied to the blades only, the coupling between two adjacent sectors due to the flexibility of the disk is zero. The theory presented here is based *a contrario* on the exact derivation of the properties of fully flexible, cyclic systems. It allows one to reduce the study of the structure to the analysis of the behavior of one of its sectors. It also shows that there exists a special relation between the spatial modes of vibration of the structure and the temporal harmonics of the excitation.

The second extension of the HFT method concerns the generation of the equations of motion derived from the Harmonic Balance Method. More precisely, a new method of condensation of the equations of motion on the set of nonlinear degrees of freedom (DOFs) is introduced. This new method, based on a modal analysis of the part of the structure that is not subject to the nonlinear forces, allows one to study without incurring time penalties systems featuring a high ratio of linear DOFs to nonlinear DOFs.

Finally, three numerical examples illustrates the capabilities of the proposed modifications of the Hybrid Frequency/Time domain method.

2. HBM FOR NON-CYCLIC STRUCTURES

The general equations of motion of a n-DOFs elastic structure are

$$\mathbf{M}\ddot{\mathbf{x}}(t) + \mathbf{C}\dot{\mathbf{x}}(t) + \mathbf{K}\mathbf{x}(t) = \mathbf{f}_l(t) + \mathbf{f}_{nl}[\mathbf{x}](t), \quad (1)$$

where $\mathbf{M}$, $\mathbf{K}$ and $\mathbf{C}$ are respectively its mass, stiffness and viscous damping matrices. $\mathbf{f}_l$ is a periodic, external force, and $\mathbf{f}_{nl}$ is an external, nonlinear force modeled as an operator acting on the displacement of the structure.

2.1 Equations of motion in complex form

When the steady-state response of the structure is assumed to be periodic, the displacement $\mathbf{x}$ and the linear force $\mathbf{f}_l$ can be written as Fourier series of harmonic functions. Assuming that keeping n_h harmonics provides an accurate approximation of the dynamics of the structure, they can be written as

$$\mathbf{x}(t) = \mathrm{Re}\Big[\sum_{k=0}^{n_h} \underline{\mathbf{x}}_k e^{-jk\omega t}\Big] \quad (2)$$

$$\mathbf{f}_l(t) = \mathrm{Re}\Big[\sum_{k=0}^{n_h} \underline{\mathbf{f}}_{l,k} e^{-jk\omega t}\Big], \quad (3)$$

where $\frac{\omega}{2\pi}$ is the frequency of excitation of $\mathbf{f}_l$. Similarly, the expression of the nonlinear force $\mathbf{f}_{nl}$ as a function of the displacement $\mathbf{x}$ is given by:

$$\mathbf{f}_{nl}[\mathbf{x}](t) = \mathrm{Re}\Big[\sum_{k=0}^{n_h} \underline{\mathbf{f}}_{nl,k}(\underline{\mathbf{x}}_0, \ldots, \underline{\mathbf{x}}_{n_h}) e^{-jk\omega t}\Big]. \quad (4)$$

Then, applying the Harmonic Balance Method to equation (1) yields a set of n_h complex, nonlinear, coupled equations

$$\underline{\mathbf{\Lambda}}_k \underline{\mathbf{x}}_k - \underline{\mathbf{f}}_{l,k} - \underline{\mathbf{f}}_{nl,k}(\underline{\mathbf{x}}_0, \ldots, \underline{\mathbf{x}}_{n_h}) = \mathbf{0}, \quad (5)$$

where

$$\underline{\mathbf{\Lambda}}_k = -(k\omega)^2\mathbf{M} + \underline{j}\, k\omega\mathbf{C} + \mathbf{K}. \quad (6)$$

2.2 Condensation of the system

Since industrial, realistic structures are in general represented by very large finite element models, it is usually not possible to solve efficiently the set of nonlinear equations (5) when the unknowns $\underline{\mathbf{x}}_k$ consist of the harmonic components of *all* the physical degrees of freedom present in the finite element (FE) model. In lieu thereof, models of significantly smaller size are used to represent the structure. Assuming that the structure's DOFs can be classified as *nonlinear* DOFs (i.e., DOFs where a nonlinear external force is applied), and *linear* DOFs (i.e., all the other DOFs of the structure), these reduced-order models are usually obtained from component mode

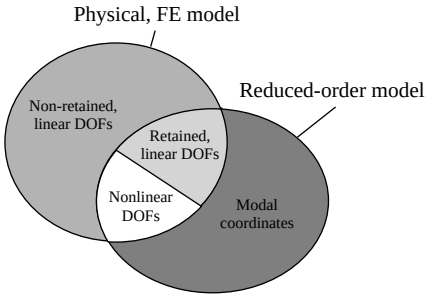

Fig. 1: Partition of physical, FE model DOFs and reduced-order model DOFs.

synthesis techniques, which substitute most of the linear DOFs of the structure by a few modal coordinates and leave the nonlinear DOFs unchanged. Therefore, when the nonlinearities are localized (i.e., the number of nonlinear DOFs is a small fraction of the total number of DOFs), significant gains in term of size are achieved.

In turbomachinery applications, such localized nonlinearities are exhibited by bladed disk assemblies with dry friction dampers attached to adjacent blades. Applying the Craig-Bampton condensation method[26] to these systems yields reduced-order models in which DOFs are partitioned as described in Fig. 1. These reduced-order models consist in:

- A subset of the physical DOFs of the original FE model. It is made of the nonlinear friction DOFs as well as any other physical DOFs (referred to as *retained, linear DOFs*) of particular importance for the analysis and the understanding of the dynamics of the structure.
- A subset of *modal coordinates* corresponding to the free vibration normal modes of the structure fixed at the retained, linear and nonlinear DOFs.

This condensation of the FE model is computationally costly and is usually done once and for all. As a consequence, when for instance parametric studies are carried out to optimize the characteristics of the dampers, it is necessary to make sure that the subset of retained physical DOFs of the reduced-order model is large enough, so that different frictional configurations can be tested without performing the condensation of the FE model for each configuration. For bladed-disk assemblies with underplatform friction dampers, one might retain for instance several candidate friction DOFs under each platform to assess the benefits of various locations of the damper. Similarly, it is usually beneficial to keep a relatively large number of normal modes so as to approximate best the dynamics of the structure.

Therefore, although the size of the reduced-order model can be several orders of magnitude smaller than the size of the original FE model, the ratio of the actual nonlinear DOFs – for a given frictional configuration – to the other DOFs of the reduced-order model (i.e., the other candidate friction DOFs not considered in this configuration, the retained linear DOFs, and the modal coordinates) can still be rather small, and makes solving the set of equations (5) difficult.

The Harmonic Balance Method provides an elegant means of reducing the system to the actual nonlinear DOFs. Let the superscript ^{r} denote the *retained* DOFs (i.e., the DOFs actually subject to a nonlinear force for a given friction configuration), and let ^{d} denote the *deleted* DOFs, i.e., all the other DOFs of the reduced-order model. Since the DOFs in the ^{d} set are not subject to a nonlinear force, the set of equations (5) can be written as

$$\begin{bmatrix} \underline{\mathbf{\Lambda}}_k^{dd} & \underline{\mathbf{\Lambda}}_k^{dr} \\ \underline{\mathbf{\Lambda}}_k^{rd} & \underline{\mathbf{\Lambda}}_k^{rr} \end{bmatrix} \begin{bmatrix} \underline{\mathbf{x}}_k^d \\ \underline{\mathbf{x}}_k^r \end{bmatrix} - \begin{bmatrix} \underline{\mathbf{f}}_{l,k}^d \\ \underline{\mathbf{f}}_{l,k}^r \end{bmatrix} - \begin{bmatrix} \mathbf{0} \\ \underline{\mathbf{f}}_{nl,k} \end{bmatrix} = \mathbf{0}. \quad (7)$$

This set of equations can be expressed as a function of $\underline{\mathbf{x}}_k^r$ only

$$\underline{\mathbf{\Lambda}}_k^{red} \underline{\mathbf{x}}_k^r - \underline{\mathbf{f}}_{l,k}^{red} - \underline{\mathbf{f}}_{nl,k}(\underline{\mathbf{x}}_0^r, \ldots, \underline{\mathbf{x}}_{n_h}^r) = \mathbf{0}, \quad (8)$$

where the reduced quantities $\underline{\mathbf{\Lambda}}_k^{red}$ and $\underline{\mathbf{f}}_{l,k}^{red}$ are defined as:

$$\underline{\mathbf{\Lambda}}_k^{red} = \underline{\mathbf{\Lambda}}_k^{rr} - \underline{\mathbf{\Lambda}}_k^{rd} \underline{\mathbf{\Lambda}}_k^{dd^{-1}} \underline{\mathbf{\Lambda}}_k^{dr} \quad (9)$$

$$\underline{\mathbf{f}}_{l,k}^{red} = \underline{\mathbf{f}}_{l,k}^r - \underline{\mathbf{\Lambda}}_k^{rd} \underline{\mathbf{\Lambda}}_k^{dd^{-1}} \underline{\mathbf{f}}_{l,k}^d. \quad (10)$$

If required, a simple backsubstitution allows one to express the value of the harmonic components of the deleted DOFs, $\underline{\mathbf{x}}_k^d$, as a function of the harmonic components of the retained nonlinear DOFs, $\underline{\mathbf{x}}_k^r$:

$$\underline{\mathbf{x}}_k^d = \underline{\mathbf{\Lambda}}_k^{dd^{-1}} [\underline{\mathbf{f}}_{l,k}^d - \underline{\mathbf{\Lambda}}_k^{dr} \underline{\mathbf{x}}_k^r]. \quad (11)$$

As a consequence of this transformation, the set of nonlinear equations (8) does not involve a combination of linear and nonlinear variables anymore. It is made of the n_h harmonic components of the n_r retained nonlinear DOFs only, resulting in a compact system of $n_r(2n_h-1)$ real, nonlinear variables*.

Traditional implementations of the HBM generate the n_h reduced matrices $\underline{\mathbf{\Lambda}}_k^{red}$ by a direct application of

* For each DOF, the coefficients of the Fourier series are complex (they are represented by a real and an imaginary part corresponding to the cosine and sine components of the series), except the coefficient corresponding to the harmonic 0, which is always real.

Eq. (9). When the response of the structure is desired over a range of frequencies, the steps described in Eqs. (9) and (10) must be repeated for each frequency. In particular, the matrices $\underline{\mathbf{\Lambda}}_k^{dd}$ have to be inverted for each value of ω, and these inversions can become very costly as the fidelity of the reduced-order model increases, i.e., as the ratio of nonlinear DOFs to deleted DOFs decreases. In some cases, the CPU time consumed by these linear operations significantly exceeds the CPU time required to solve the condensed, nonlinear problem.

The reduced matrices $\underline{\mathbf{\Lambda}}_k^{red}$ can be generated in a simple way which alleviates this problem. Assuming that the damping matrix $\mathbf{C}$ is proportional to the mass and stiffness matrices of the structure, that is,

$$\mathbf{C} = \alpha\mathbf{K} + \beta\mathbf{M}, \tag{12}$$

and defining the complex scalars $\underline{\varepsilon}_k$ and $\underline{\delta}_k$ as

$$\underline{\varepsilon}_k = 1 + \underline{j}k\omega\alpha \tag{13}$$

$$\underline{\delta}_k = -(k\omega)^2 + \underline{j}k\omega\beta, \tag{14}$$

$\underline{\mathbf{\Lambda}}_k^{dd}$ can be written as

$$\underline{\mathbf{\Lambda}}_k^{dd} = \underline{\varepsilon}_k\mathbf{K}^{dd} + \underline{\delta}_k\mathbf{M}^{dd}, \tag{15}$$

with similar expressions available for $\underline{\mathbf{\Lambda}}_k^{rr}$, $\underline{\mathbf{\Lambda}}_k^{rd}$ and $\underline{\mathbf{\Lambda}}_k^{dr}$. Then, solving the eigenproblem

$$[\mathbf{K}^{dd} + \lambda\mathbf{M}^{dd}]\mathbf{x}^d = \mathbf{0} \tag{16}$$

yields

$$\mathbf{M}^{dd^{-1}}\mathbf{K}^{dd} = \mathbf{P}\mathbf{D}\mathbf{P}^{-1}, \tag{17}$$

where $\mathbf{D}$ is a diagonal matrix. Now, defining the diagonal matrices $\underline{\mathbf{\Theta}}_k$ as

$$\underline{\mathbf{\Theta}}_k = \underline{\varepsilon}_k\mathbf{D} + \underline{\delta}_k\mathbf{I}, \tag{18}$$

where $\mathbf{I}$ is the identity matrix, and combining Eqs. (15), (17) and (18), one obtains the following expression for the inverse of $\underline{\mathbf{\Lambda}}_k^{dd}$:

$$\underline{\mathbf{\Lambda}}_k^{dd^{-1}} = \mathbf{P}\underline{\mathbf{\Theta}}_k^{-1}\mathbf{P}^{-1}\mathbf{M}^{dd^{-1}}. \tag{19}$$

Introducing the constant matrices $\mathbf{U}$, $\mathbf{U}'$, $\mathbf{V}$, and $\mathbf{V}'$ defined as

$$\mathbf{U} = \mathbf{K}^{rd}\mathbf{P} \tag{20}$$

$$\mathbf{U}' = \mathbf{M}^{rd}\mathbf{P} \tag{21}$$

$$\mathbf{V} = \mathbf{P}^{-1}\mathbf{M}^{dd^{-1}}\mathbf{K}^{dr} \tag{22}$$

$$\mathbf{V} = \mathbf{P}^{-1}\mathbf{M}^{dd^{-1}}\mathbf{M}^{dr}, \tag{23}$$

and substituting these expressions in equation (9), the reduced matrices $\underline{\mathbf{\Lambda}}_k^{red}$ can finally be expressed as:

$$\begin{aligned}\underline{\mathbf{\Lambda}}_k^{red} = \underline{\mathbf{\Lambda}}_k^{rr} &- \mathbf{U}[\underline{\varepsilon}_k^2\underline{\mathbf{\Theta}}_k^{-1}\mathbf{V} + \underline{\varepsilon}_k\underline{\delta}_k\underline{\mathbf{\Theta}}_k^{-1}\mathbf{V}'] \\ &- \mathbf{U}'[\underline{\delta}_k\underline{\varepsilon}_k\underline{\mathbf{\Theta}}_k^{-1}\mathbf{V} + \underline{\delta}_k^2\underline{\mathbf{\Theta}}_k^{-1}\mathbf{V}'].\end{aligned} \tag{24}$$

The advantage of this formulation is that $\mathbf{U}$, $\mathbf{U}'$, $\mathbf{V}$, and $\mathbf{V}'$ can be computed once and for all (they are independent of ω), and that the inversion of the matrices $\underline{\mathbf{\Lambda}}_k^{dd}$ is replaced by the trivial inversion of the diagonal, complex matrices $\underline{\mathbf{\Theta}}_k$. When large models are considered (e.g., mistuned bladed disk assemblies with as many friction dampers as blades), significant CPU-time gains ensue.

3. HBM FOR CYCLIC STRUCTURES

Unlike the general structures described in the previous section, a typical friction damped, bladed disk is a structure which exhibits a cyclic symmetry, that is, the geometry of the complete assembly (i.e., the disk, the blades and the underplatform dampers) can be deduced by successive rotations of one of its sectors. Such a structure can be fully described by (1) the geometry and the mechanical properties of a single sector, and (2) the number of sectors n_s of the assembly.

As the bladed disk rotates, it is subject to a constant, non-uniform pressure field, and the variations of pressure experienced by the sectors due to the rotation of the structure result in a vibratory response of the assembly.

3.1 Temporal periodicity of the response

For the sake of clarity, we introduce the two following reference frames:

- (R) is a reference frame fixed with respect to the structure. In this reference frame, the position of a point Q of the structure is expressed in polar coordinates as $Q(r, \alpha, z)$, where z corresponds to the axis of rotation of the disk.
- (R') is a reference frame fixed with respect to the pressure field. The position of a point Q' fixed with respect to (R') is expressed in polar coordinates as $Q'(r, \theta, z)$.

It is somehow more convenient to carry out the analysis of the response of the structure by considering that the disk is fixed in space and that the pressure field rotates, resulting in a travelling excitation which excites the bladed disk assembly, as shown in Fig. 2.

Since the pressure field is time invariant in (R'), the pressure observed at any point $Q'(r, \theta, z)$ fixed in (R') can be described by an infinite Fourier series:

$$P(Q') = \mathrm{Re}\Big[\sum_{k=0}^{\infty}\underline{p}_k(r, z)e^{-jk\theta}\Big]. \tag{25}$$

In most turbomachinery applications however, the pressure field features a spatial periodicity defined by an integer e_o, referred to as "engine order". That is, the pressure

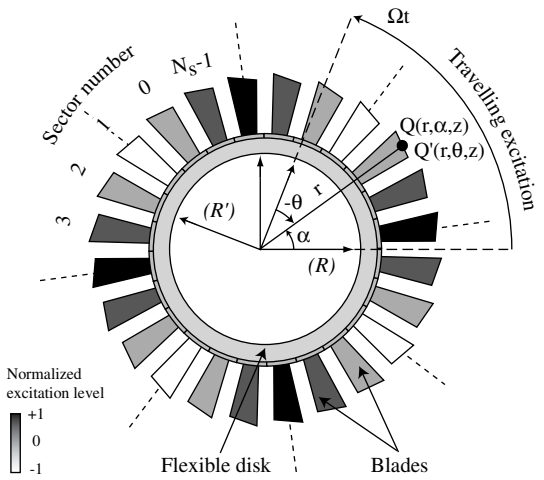

Fig. 2: Example of structure with cyclic symmetry.

field can be fully described by any angular sector of size $2\pi/e_o$ repeated e_o times, and $P\big(Q'\big)$ is given by:

$$P\big(Q'\big) = \mathrm{Re}\big[\sum_{k=0}^{\infty} \underline{p}_k(r,z)e^{-jke_o\theta}\big]. \tag{26}$$

Figure 2 shows an example of travelling excitation when e_o – also referred to as the number of nodal diameters of the excitation – is equal to 4.

Now, defining Ω as the angular velocity of (R') with respect to (R), and assuming that the two reference frames coincide at $t = 0$, the angular coordinates of two points Q (fixed in (R)) and Q' (fixed in (R')) coinciding at t must satisfy:

$$\theta = \Omega t - \alpha. \tag{27}$$

As a consequence, the pressure observed at t at a fixed point $Q(r,\alpha)$ of the structure is expressed as:

$$P\big(Q,t\big) = \mathrm{Re}\big[\sum_{k=0}^{\infty} \underline{p}_k(r,z)e^{-jke_o(\Omega t-\alpha)}\big]. \tag{28}$$

Then, defining ω as

$$\omega = \Omega e_o, \tag{29}$$

and integrating Eq. (28) over the elements of the structure, one obtains the expression of the linear, travelling excitation in the reference frame (R):

$$\tilde{\mathbf{f}}_l(t) = \mathrm{Re}\big[\sum_{k=0}^{\infty} \tilde{\underline{\mathbf{f}}}_{l,k}e^{-jk\omega t}\big]. \tag{30}$$

Thus, the spatial harmonics which define the constant, rotating pressure field correspond to the temporal harmonics of the linear excitation acting on the bladed disk, and the pulsation of the fundamental temporal harmonic of $\tilde{\mathbf{f}}_l$ is ω.

Now, assuming that gyroscopic effects are neglected, the equations of motions of the complete structure can be expressed as

$$\tilde{\mathbf{M}}\ddot{\tilde{\mathbf{x}}}(t) + \tilde{\mathbf{C}}\dot{\tilde{\mathbf{x}}}(t) + \tilde{\mathbf{K}}\tilde{\mathbf{x}}(t) = \tilde{\mathbf{f}}_l(t) + \tilde{\mathbf{f}}_{nl}[\tilde{\mathbf{x}}](t), \tag{31}$$

where $\tilde{}$ indicates that the variable refers to *all* the $\tilde{n}$ DOFs of the structure, $\tilde{n}$ being defined as the product of n_s by the number n of DOFs per sector. As in the previous section, $\tilde{\mathbf{f}}_{nl}$ represents the nonlinear forces due to the friction dampers.

Labeling the n_s sectors of the assembly as indicated in Fig. 2, the displacement of the structure as well as the linear and nonlinear forces can be written as

$$\tilde{\mathbf{x}}(t) = \big[\mathbf{x}^{0^T}(t), \ldots, \mathbf{x}^{n_s-1^T}(t)\big]^T \tag{32}$$

$$\tilde{\mathbf{f}}_l(t) = \big[\mathbf{f}_l^{0^T}(t), \ldots, \mathbf{f}_l^{n_s-1^T}(t)\big]^T \tag{33}$$

$$\tilde{\mathbf{f}}_{nl}[\tilde{\mathbf{x}}](t) = \big[\mathbf{f}_{nl}^{0^T}[\tilde{\mathbf{x}}](t), \ldots, \mathbf{f}_{nl}^{n_s-1^T}[\tilde{\mathbf{x}}](t)\big]^T, \tag{34}$$

and in the following, the sector numbered "0" will be referred to as *reference* sector.

Since $\tilde{\mathbf{f}}_l$ corresponds to a wave rotating at the angular velocity Ω, the external excitations applied at time t to two adjacent sectors differ only by a simple temporal phase ϕ_t, defined as:

$$\phi_t = \frac{2\pi}{\Omega n_s}. \tag{35}$$

Thus, the excitation applied to the q-th sector of the assembly can be fully deduced from the excitation applied to the reference sector:

$$\mathbf{f}_l^q(t) = \mathbf{f}_l^0(t - q\phi_t). \tag{36}$$

Now, assuming that the response of the structure exhibits the same temporal phase, the displacement of the whole structure can also be expressed as a function of the displacement of the reference sector, that is,

$$\mathbf{x}^q(t) = \mathbf{x}^0(t - q\phi_t). \tag{37}$$

As a consequence, the definition of the nonlinear forces $\mathbf{f}_{nl}^q$ as operators acting on $\tilde{\mathbf{x}}$ can be modified so as to involve $\mathbf{x}^0$ only,

$$\mathbf{f}_{nl}^q[\tilde{\mathbf{x}}](t) = \mathbf{f}_{nl}^q[\mathbf{x}^0](t), \tag{38}$$

and the phase relation (37) yields:

$$\mathbf{f}_{nl}^q[\tilde{\mathbf{x}}](t) = \mathbf{f}_{nl}^0[\mathbf{x}^0](t - q\phi_t). \tag{39}$$

3.2 Equations of motion in complex form

Since the pulsation of the excitation $\tilde{\mathbf{f}}_l$ is ω, and assuming that n_h-harmonic Fourier series are accurate enough to approximate the dynamics of the structure, the phase relations (36), (37) and (39) allows one to write in complex form $\tilde{\mathbf{x}}$, $\tilde{\mathbf{f}}_l$, and $\tilde{\mathbf{f}}_{nl}$ as:

$$\begin{aligned}\underline{\tilde{\mathbf{x}}}(t) = \sum_{k=0}^{n_h} \big[&\underline{\mathbf{x}}_k^{0^T} e^{-jk\omega t}, \dots \\ &\dots, \underline{\mathbf{x}}_k^{0^T} e^{-jk\omega (t-(n_s-1)\phi_t)}\big]^T,\end{aligned} \tag{40}$$

$$\begin{aligned}\underline{\tilde{\mathbf{f}}}_l(t) = \sum_{k=0}^{n_h} \big[&\underline{\mathbf{f}}_{l,k}^{0^T} e^{-jk\omega t}, \dots \\ &\dots, \underline{\mathbf{f}}_{l,k}^{0^T} e^{-jk\omega (t-(n_s-1)\phi_t)}\big]^T,\end{aligned} \tag{41}$$

and

$$\begin{aligned}\underline{\tilde{\mathbf{f}}}_{nl}[\tilde{\mathbf{x}}](t) = \sum_{k=0}^{n_h} \big[&\underline{\mathbf{f}}_{nl,k}^{0^T}(\underline{\mathbf{x}}_0^0, \dots, \underline{\mathbf{x}}_{n_h}^0) e^{-jk\omega t}, \dots \\ &\dots, \underline{\mathbf{f}}_{nl,k}^{0^T}(\underline{\mathbf{x}}_0^0, \dots, \underline{\mathbf{x}}_{n_h}^0) e^{-jk\omega (t-(n_s-1)\phi_t)}\big]^T.\end{aligned} \tag{42}$$

These equations can be written in a more compact form,

$$\underline{\tilde{\mathbf{x}}}(t) = \sum_{k=0}^{n_h} \big[\underline{\mathbf{u}}_k^{e_o} \otimes \underline{\mathbf{x}}_k^0\big] e^{-jk\omega t} \tag{43}$$

$$\underline{\tilde{\mathbf{f}}}_l(t) = \sum_{k=0}^{n_h} \big[\underline{\mathbf{u}}_k^{e_o} \otimes \underline{\mathbf{f}}_{l,k}^0\big] e^{-jk\omega t} \tag{44}$$

$$\underline{\tilde{\mathbf{f}}}_{nl}[\tilde{\mathbf{x}}](t) = \sum_{k=0}^{n_h} \big[\underline{\mathbf{u}}_k^{e_o} \otimes \underline{\mathbf{f}}_{nl,k}^0(\underline{\mathbf{x}}_0^0, \dots, \underline{\mathbf{x}}_{n_h}^0)\big] e^{-jk\omega t}, \tag{45}$$

where the Kronecker product $\otimes$ and the vector $\underline{\mathbf{u}}_k^{e_o}$ are defined in the appendix.

Then, using Eqs. (43-45), introducing the matrices $\underline{\tilde{\mathbf{\Lambda}}}_k$ as

$$\underline{\tilde{\mathbf{\Lambda}}}_k = -(k\omega)^2 \tilde{\mathbf{M}} + \underline{j} k\omega \tilde{\mathbf{C}} + \tilde{\mathbf{K}}, \tag{46}$$

and applying the harmonic balance method to Eq. (31), one obtains:

$$\begin{aligned}&\underline{\tilde{\mathbf{\Lambda}}}_k(\underline{\mathbf{u}}_k^{e_o} \otimes \underline{\mathbf{x}}_k^0) - \underline{\mathbf{u}}_k^{e_o} \otimes \underline{\mathbf{f}}_{l,k}^0 \\ &\quad - \underline{\mathbf{u}}_k^{e_o} \otimes \underline{\mathbf{f}}_{nl,k}^0(\underline{\mathbf{x}}_0^0, \dots, \underline{\mathbf{x}}_{n_h}^0) = \mathbf{0}.\end{aligned} \tag{47}$$

The last step in this analysis is based on the definition and properties of the extended Fourier matrix presented in the appendix. In particular, since the bladed disk is spatially cyclic, (i.e., $\tilde{\mathbf{M}}$, $\tilde{\mathbf{K}}$ and $\tilde{\mathbf{C}}$ are block-circulant matrices), the trivial transformation

$$\begin{aligned}&\underline{\tilde{\mathbf{E}}}^* \underline{\tilde{\mathbf{\Lambda}}}_k \underline{\tilde{\mathbf{E}}} \underline{\tilde{\mathbf{E}}}^* (\underline{\mathbf{u}}_k^{e_o} \otimes \underline{\mathbf{x}}_k^0) - \underline{\tilde{\mathbf{E}}}^* (\underline{\mathbf{u}}_k^{e_o} \otimes \underline{\mathbf{f}}_{l,k}^0) \\ &\quad - \underline{\tilde{\mathbf{E}}}^* (\underline{\mathbf{u}}_k^{e_o} \otimes \underline{\mathbf{f}}_{nl,k}^0(\underline{\mathbf{x}}_0^0, \dots, \underline{\mathbf{x}}_{n_h}^0)) = \mathbf{0}\end{aligned} \tag{48}$$

Temporal harmonic

Engine order	0	1	2	3	4	5	6	7	8	9	10	11	12	13	...
0	0	0	0	0	0	0	0	0	0	0	0	0	0	0	...
1	0	1	2	3	4	5	6	7	8	9	10	11	12	0	...
2	0	2	4	6	8	10	12	1	3	5	7	9	11	0	...
3	0	3	6	9	12	2	5	8	11	1	4	7	10	0	...
4	0	4	8	12	3	7	11	2	6	10	1	5	9	0	...
5	0	5	10	2	7	12	4	9	1	6	11	3	8	0	...
6	0	6	12	5	11	4	10	3	9	2	8	1	7	0	...

Spatial harmonic

Table 1: Relation between the *spatial harmonics* of the response of a 13-sector cyclic structure and the *temporal harmonics* of the excitation applied to one of its sectors, for various engine orders.

yields the block-diagonal form of Eq. (47):

$$\begin{aligned}&\mathbf{BDiag}[\underline{\mathbf{\Lambda}}_k^0, \dots, \underline{\mathbf{\Lambda}}_k^{n_s-1}](\underline{\mathbf{E}}^* \otimes \mathbf{I}_n)(\underline{\mathbf{u}}_k^{e_o} \otimes \underline{\mathbf{x}}_k^0) \\ &- (\underline{\mathbf{E}}^* \otimes \mathbf{I}_n)(\underline{\mathbf{u}}_k^{e_o} \otimes \underline{\mathbf{f}}_{l,k}^0) \\ &- (\underline{\mathbf{E}}^* \otimes \mathbf{I}_n)(\underline{\mathbf{u}}_k^{e_o} \otimes \underline{\mathbf{f}}_{nl,k}^0(\underline{\mathbf{x}}_0^0, \dots, \underline{\mathbf{x}}_{n_h}^0)) = \mathbf{0},\end{aligned} \tag{49}$$

where

$$\underline{\mathbf{\Lambda}}_k^q = -(k\omega)^2 \underline{\mathbf{M}}^q + \underline{j} k\omega \underline{\mathbf{C}}^q + \underline{\mathbf{K}}^q. \tag{50}$$

Then, the distributivity property of the Kronecker product allows one to rewrite Eq. (49) as:

$$\begin{aligned}&\mathbf{BDiag}[\underline{\mathbf{\Lambda}}_k^0, \dots, \underline{\mathbf{\Lambda}}_k^{n_s-1}](\underline{\mathbf{E}}^* \underline{\mathbf{u}}_k^{e_o}) \otimes \underline{\mathbf{x}}_k^0 \\ &- (\underline{\mathbf{E}}^* \underline{\mathbf{u}}_k^{e_o}) \otimes \underline{\mathbf{f}}_{l,k}^0 \\ &- (\underline{\mathbf{E}}^* \underline{\mathbf{u}}_k^{e_o}) \otimes \underline{\mathbf{f}}_{nl,k}^0(\underline{\mathbf{x}}_0^0, \dots, \underline{\mathbf{x}}_{n_h}^0)) = \mathbf{0}.\end{aligned} \tag{51}$$

Finally, the property of the product $\underline{\mathbf{E}}^* \underline{\mathbf{u}}_k^{e_o}$ explained in the appendix yields the most compact form of the n_h equations of motion:

$$\underline{\mathbf{\Lambda}}_k^{q(k,e_o)} \underline{\mathbf{x}}_k^0 - \underline{\mathbf{f}}_{l,k}^0 - \underline{\mathbf{f}}_{nl,k}^0(\underline{\mathbf{x}}_0^0, \dots, \underline{\mathbf{x}}_{n_h}^0) = \mathbf{0}, \tag{52}$$

where

$$q(k, e_o) - k e_o \equiv 0 \; [n_s]. \tag{53}$$

If required, this set of nonlinear equations can be reduced to the nonlinear DOFs of the reference sector, in a fashion strictly similar to the method previously presented.

3.3 Comments

Although the set of nonlinear equations (52) obtained for a cyclic system shares many similarities with the set of equations (5) obtained in the general, non-cyclic case, some important differences should be noted:

- The unknowns involved in the set of equations (52) consist of the Fourier coefficients of the DOFs of the reference sector only. They represent the actual motion of the nodes of the reference sector. The gain in terms of reduction of the size of the nonlinear system is therefore extremely important, since the DOFs of the other sectors can be ignored.

- A simple temporal phase ϕ_t exists between the response of two adjacent sectors. This phase relation applies to the displacement of the structure, the linear and the nonlinear forces as well, and it depends on (1) the pulsation ω of the linear excitation applied on the reference sector, (2) the spatial repetitivity e_o of the travelling excitation; and (3), the number of sectors n_s of the assembly. ϕ_t is given by:

$$\phi_t = \frac{2\pi}{\omega e_o n_s}. \tag{54}$$

- Although the nonlinear force applied to the reference sector depends on the DOFs of this sector as well as the DOFs of other sectors of the assembly - as it is the case for underplatform friction dampers which straddle consecutive sectors – it can be expressed as a function of the motion of the reference DOFs only.

- The matrices $\underline{\mathbf{M}}^q$, $\underline{\mathbf{K}}^q$ and $\underline{\mathbf{C}}^q$ appearing in the definition of the matrices $\underline{\mathbf{\Lambda}}_k^q$ are complex, and they represent the structural matrices associated to the natural modes of vibrations of the reference sector when the response of the complete structure exhibits a spatial cyclicity of order q. Since the complete structure features n_s sectors, the maximum value of q is $n_s - 1$.

The set of equations (52) is best understood by realizing that the nonlinear response of the complete structure is actually approximated by a finite series of linear responses. The set of nonlinear equations (52) is indeed made of n_h coupled linear systems, where each linear system corresponds to the equations of motion of the reference sector when the complete cyclic structure is subject to a mono-harmonic travelling wave. The nonlinearity of the complete set of equations stems from the coupling of the solutions of these linear systems by the nonlinear force.

For instance, for the linear system associated to $k = 1$, the structure is subject to a rotating, mono-harmonic travelling wave of spatial cyclicity e_0, or, in other words, the structure is subject to a rotating wave made of the spatial harmonic e_o only. The response of the structure is therefore a travelling wave of same characteristics, i.e., it features the spatial harmonic e_o only. This response is obtained for the reference sector – from which the response over all the assembly can be deduced – by selecting the structural matrices $\underline{\mathbf{M}}^1$, $\underline{\mathbf{K}}^1$, and $\underline{\mathbf{C}}^1$ which correspond to the modes of vibrations with one nodal diameter.

As long as the inequality $ke_o < n_s$ is verified, the spatial harmonic of the response matches exactly the spatial harmonic of the travelling excitation. However, when $ke_o \geq n_s$, the response of the structure cannot exhibit a spatial cyclicity of ke_o, since it is made of n_s sectors. Instead, the response of the structure exhibits a spatial harmonic $q(k, e_o)$, where $q(k, e_o)$ is defined in Eq. (53). Eq. (53) is of course also valid when ke_o is lower than n_s.

Since the spatial harmonic waves of the excitation are each associated to a temporal harmonic of the forcing applied to the reference sector, Eq. (53) can therefore be understood as the relation between the temporal harmonics of the linear and nonlinear forces applied to the reference sector, and the spatial harmonics present in the response of the complete structure. This relation is illustrated in Table 1 for a 13-sector cyclic structure.

One should also note that although the linear excitation $\mathbf{f}_l^0(t)$ is approximated by a relatively low number of harmonics – less than 3 in general –, the nonlinear force $\mathbf{f}_{nl}^0[\mathbf{x}^0](t)$ has usually a much richer harmonic content. As a consequence, the number of spatial harmonics which are present in the response of the structure is in most cases not limited by the number of temporal harmonics, and it is determined by e_o and n_s only. For instance, considering a 160-sector assembly subject to a force featuring 64 nodal diameters, the only spatial harmonics potentially present are: 0, 32, 64, 128, and 96.

4. SOLUTION METHOD

As mentioned above, the equations of motion of both cyclic and non-cyclic structures are governed by a set of n_h similar matrix equations. They can also be written in real form and combined into a single nonlinear matrix equation, so that the harmonic coefficients that describe the dynamics of the system are solution of a nonlinear function $\mathbf{F}$, defined as

$$\mathbf{F}(\mathbf{u}) = \mathbf{\Lambda}\mathbf{u} - \mathbf{f} - \mathbf{f}_{nl}(\mathbf{u}), \tag{55}$$

where $\mathbf{u}$ consists of the harmonic cosine and sine coefficients of the motion of all or part of the nonlinear DOFs of the structure (depending on whether it is cyclic or not).

4.1 Hybrid Frequency/Time domain method

The nonlinear equation $\mathbf{F}(\mathbf{u}) = \mathbf{0}$ is solved using a nonlinear solver based on an implementation of the hy-

brid Powell algorithm[27] proposed by Garbow *et al*[28] . Given an initial approximation $\mathbf{u}^{(0)}$ of the solution, this algorithm generates successive estimations $\mathbf{u}^{(1)}$, $\mathbf{u}^{(2)}$, ..., $\mathbf{u}^{(m)}$, until satisfactory convergence of this series towards the solution is detected. This algorithm requires one to evaluate the nonlinear function $\mathbf{F}$ and its jacobian $\mathbf{J}$ for any input motion $\mathbf{u}$.

In the Hybrid Frequency/Time domain method, this evaluation is performed by applying to the displacement and the nonlinear force alternate transformations from the frequency domain to the time domain. Its principal steps are outlined as follows:

1. Inverse Fast Fourier Transforms are applied to the harmonic coefficients stored in $\mathbf{u}$, so as to obtain the periodic time histories of the motion of the nonlinear DOFs of the structure.

2. The time histories of the nonlinear forces resulting from this imposed displacement are calculated.

3. Fast Fourier Transforms are applied to the time histories of the nonlinear forces, and they yield the harmonic coefficients stored in $\mathbf{f}_{nl}(\mathbf{u})$.

4. $\mathbf{F}(\mathbf{u})$ is evaluated according to Eq. (55).

The advantage of the HFT method is that the evaluation of the nonlinear forces is performed in the time domain. Therefore, the nonlinearities associated to these forces can be calculated with a very high accuracy. Also, evaluating these forces in the time domain allows one to capture complex hysteretic nonlinearities, such as the stick/slip behavior of friction dampers.

As a consequence, the accuracy of the HFT method is only limited by (1) the number of harmonics used in the HBM to generate the equations of motion, and (2), the ability of the nonlinear solver to converge towards the solution.

4.2 Structures with multiple frictional interfaces

For structures featuring several frictional interfaces, that is, non-cyclic structures with several friction dampers attached, or cyclic structures which feature more than one friction damper per sector, the jacobian of Eq. (55) can be computed in a very efficient way. Mistuned bladed disks are examples of such structures: since they do not satisfy the cyclic symmetry hypothesis, their dynamics cannot be deduced from the study of one sector only, and therefore their analysis must consider the complete assembly and all the friction dampers.

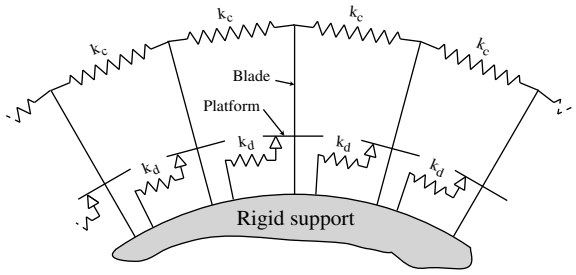

Fig. 3: Partial view of a bladed disk assembly model.

For such systems, the components of $\mathbf{u}$ can be ordered as:

$$\mathbf{u} = \left\{ \mathbf{u}^{1^T}, \ldots, \mathbf{u}^{n_d^T} \right\}^T, \tag{56}$$

where $\mathbf{u}^p$ consists of the cosine and sine harmonic coefficients of the nonlinear DOFs corresponding to the p-th friction damper, that is:

$$\mathbf{u}^p = \left\{ \mathbf{u}_0^{p^T}, \mathbf{u}_{1,c}^{p^T}, \mathbf{u}_{1,s}^{p^T}, \ldots, \mathbf{u}_{n_h,c}^{p^T}, \mathbf{u}_{n_h,s}^{p^T} \right\}^T. \tag{57}$$

Since the nonlinear friction forces exerted by the dampers depend on the motion of the corresponding frictional interfaces only, $\mathbf{f}_{nl}$ is expressed as:

$$\mathbf{f}_{nl}(\mathbf{u}) = \left\{ \mathbf{f}_{nl}^{1^T}(\mathbf{u}^1), \ldots, \mathbf{f}_{nl}^{n_d{}^T}(\mathbf{u}^{n_d}) \right\}^T. \tag{58}$$

Thus, the jacobian of the nonlinear function $\mathbf{F}$ is given by:

$$\mathbf{J} = \mathbf{\Lambda} - \mathbf{BDiag}\left[\mathbf{J}^1, \ldots, \mathbf{J}^{n_d}\right], \tag{59}$$

where

$$\mathbf{J}^p = \frac{\partial \mathbf{f}_{nl}^p(\mathbf{u}^p)}{\partial \mathbf{u}^p}. \tag{60}$$

$\mathbf{\Lambda}$ is the linear part of the jacobian. As observed in the derivation of the equations of motion obtained by the harmonic balance method, it depends only on the structural matrices and the frequency of excitation ω.

Therefore, when Eq. (55) is solved for a given frequency, $\mathbf{\Lambda}$ can be computed once and for all at the beginning of the solution process. If the nonlinear solver needs a new estimate of the jacobian as it converges towards the solution, $\mathbf{\Lambda}$ does not need to be recalculated, and only a new, simple evaluation of the blocks $\mathbf{J}^p$ is necessary. These blocks are easily calculated by finite differences with successive evaluations of the nonlinear functions $\mathbf{f}_{nl}^p$.

Thus, when n_d is very large, namely, when the structure features a large number of independent frictional interfaces, $\mathbf{J}$ is obtained in a very efficient fashion that does not penalize, in terms of CPU time, the solving of the nonlinear function $\mathbf{F}$.

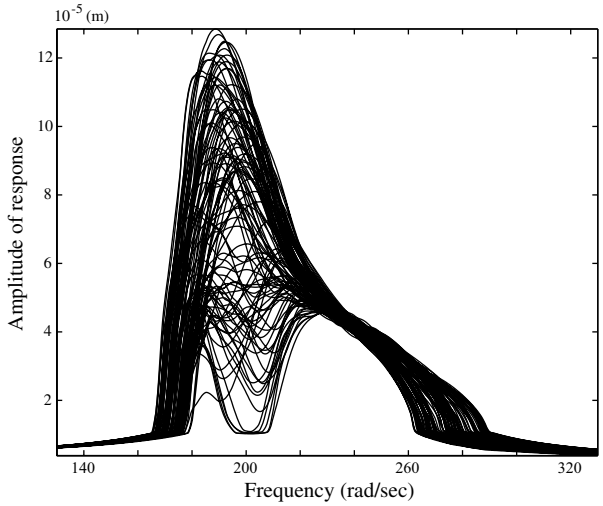

Fig. 4: Forced response of the nonlinear friction DOFs of a 7% mistuned, 108 beam assembly. The response of the structure is approximated with the harmonics 1, 3, 5, . . ., 21.

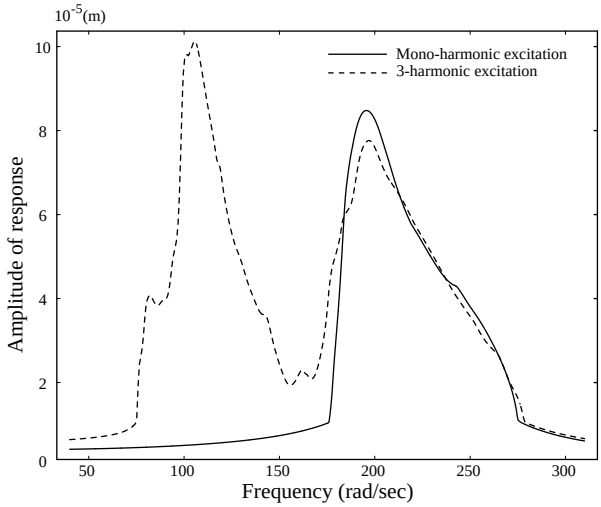

Fig. 5: Forced response of the nonlinear friction DOF of the reference sector of a 36-beam cyclic assembly. 21 harmonics are retained to describe the dynamics of the structure.

5. NUMERICAL EXAMPLES

Three numerical examples are presented in this paper. They illustrate the ability of the Hybrid Frequency/Time domain method to handle efficiently (1) structures with a high number of nonlinear DOFs, (2) cyclic structures; and (3), systems where the time histories of the nonlinear forces are complicated.

5.1 Mistuned bladed disk assembly

In this example, a structure made of 108 beams with 108 ground-to-blade friction dampers is considered. The forced response of a system of 36 beams with similar characteristics has been studied by Nacivet *et al.*[23,24] . As partially depicted in Fig. 3, the beams of this system are attached to a fixed, rigid support. The mass and stiffness matrices of the i-th beam are defined as:

$$\mathbf{M}_i = \mathbf{M}$$
$$\mathbf{K}_i = \delta_i \mathbf{K},$$

where $\mathbf{M}$ and $\mathbf{K}$ are 3-by-3 matrices provided by SNECMA Co., which correspond to a reduced-order model of blade described in Berthillier *et al.*[29] The mistuning coefficients δ_i follow a normal distribution centered at 1 with a standard deviation of 7%.

A stiffness k_c of 4.5×10^3 N couples the tips of two adjacent beams. This stiffness can be interpreted as the flexibility of the disk or as a shroud for more realistic bladed-disk assemblies.

Each beam is subject to the action of a ground-to-blade friction damper, and all the dampers share the same characteristics. They are modeled as simple hysteretic dampers of stiffness $k_d = 2.4 \times 10^7$ N.m^{-1}. They follow the law of dry friction of Coulomb, with a friction coefficient of 1. The contact point at the platform/damper interface is allowed to move along one direction, and the dampers are pressed under the platforms with a constant normal load of 250 N. Therefore, the dampers exert a nonlinear friction force on only one DOF of each of the beams.

Finally, the tips of the beams are subject to a mono-harmonic traveling excitation of amplitude 20 N with an engine order of 5.

The forced response of the structure is depicted in Fig. 4. The characteristics of the set of equations solved by the HFT method are given below:

- The structure is represented by 324 DOFs, among which 108 are nonlinear.
- The forced response of the system has been calculated with the harmonics 1, 3, 5, 7,. . ., 19 and 21, since it can be proven that the even harmonics of the friction forces are exactly zero for the type of nonlinearity considered here. Therefore, the motion of each DOF is represented by 22 real coefficients.

As a consequence, the dynamics of the structure is represented by 7128 harmonic coefficients, which lead to a reduced nonlinear system of 2376 unknowns, correspond-

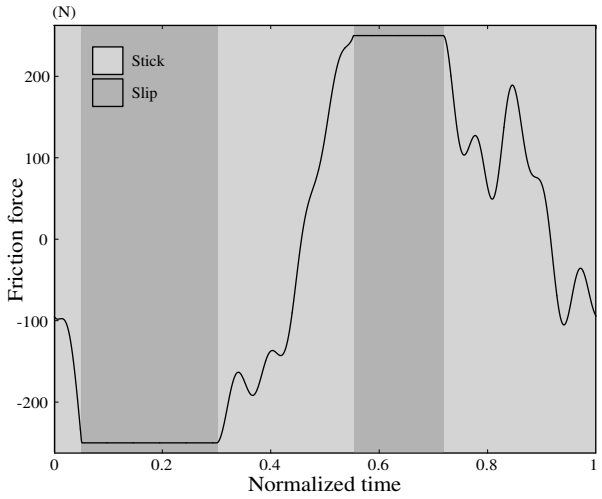

Fig. 6: Time history of the friction force applied to the nonlinear DOF of the reference sector at 200 rad.s^{-1}.

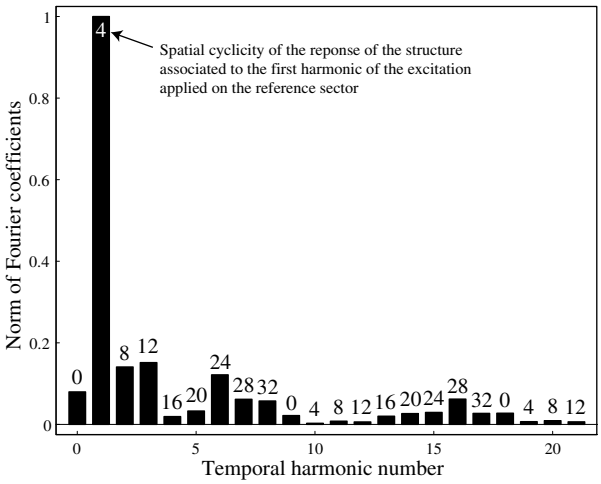

Fig. 7: Temporal harmonics of the nonlinear force applied to the reference sector, with the corresponding spatial harmonics exhibited by the response of the structure.

ing to the harmonic coefficients of the nonlinear DOFs only.

A Gateway computer with a 2 GHz Pentium IV processor has been used to calculate this forced response. The CPU time required to solve the nonlinear system near the resonant peak at 200 rad.s^{-1} is 110 seconds. At the same frequency, the CPU time dedicated to the condensation of the system on the nonlinear DOFs represents about 1.5 second. This means that the number of linear DOFs of the structure could be greatly increased without penalizing the CPU time required to solve the nonlinear system. In particular, a greater number of normal modes could be included in the reduced-order models that represent the beams so as to increase the accuracy of the calculation.

This study shows that the HFT method is applicable to the calculation of the forced response of systems having a large number of nonlinear friction DOFs, without sacrificing the number of harmonics retained in the analysis.

5.2 Tuned bladed disk assembly

The characteristics of the structure presented in the first example are now slightly modified: The number of beams of the assembly is reduced to 36, and the mistuning coefficients δ_i are all set to 0, so that the structure is spatially cyclic. Therefore, the cyclic symmetry theory developed in this paper can be directly applied to the structure. The properties of the dampers as well as the value of the inter-sector elastic coupling remain unchanged.

The forced response of the structure is studied for two different excitations. The first excitation is a travelling wave of engine order $e_o = 4$, which rotates with the angular velocity Ω. It is approximated by a series of three spatial harmonics of cyclicity e_o, $2e_o$ and $3e_o$. As these waves rotate, they excite the reference sector of the structure at the pulsations ω, 2ω and 3ω, where $\omega = e_o\Omega$. The first linear excitation applied to the tip of the beam of the reference sector is therefore defined as:

$$f_l^1(t) = 20\cos(\omega t) + 15\sin(2\omega t) + 4\cos(3\omega t) + 3\sin(3\omega t)$$

One should note that the amplitudes of the second and third harmonic waves are designed so that they correspond respectively to 75% and 25% of the amplitude of the fundamental wave. These values are common in turbomachinery applications.

The second excitation studied is simply the mono-harmonic approximation of the first one, that is:

$$f_l^2(t) = 20\cos(\omega t).$$

For these two excitations, the forced responses of the friction DOF of the reference sector have been computed with the harmonics 0, 1, 2, ..., 20 and 21. The comparison of these two responses is shown in Fig. 5. It illustrates the dramatic change of behavior of the system when one neglects to take into account all the harmonics of the linear excitation.

When subject to a mono-harmonic excitation, the structure exhibits a response with only one resonant peak, around 200 rad/s. When subject to the three-harmonic excitation, a second resonant peak appears around 100 rad/s. This peak is due to the presence of

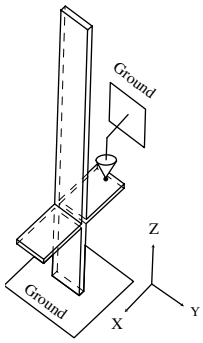

Length = 1.0 m
Width = 0.08 m
Thickness = 0.02 m
Young's modulus = 2.0 10^{11} Pa
Poisson ratio = 0.3
Density = 7600 kg/m^3

The platforms are located at one fourth of the beam, and are 0.10 m long.

The friction point is centered at 0.02 m of the free edge of the platform

Fig. 8: Model of cantilevered beam with attached friction damper.

the second spatial harmonic of engine order $2e_o$, which excites the reference sector at twice the frequency of the fundamental temporal harmonic. One should also expect a third resonant peak around 70 rad/s; however, the amplitude of the third harmonic of the excitation is not large enough to produce a significant contribution in the response, and the response of the structure at this frequency is largely dominated by the second component of the excitation.

Figure 6 shows the time history of the friction force applied to the nonlinear DOF of the reference sector. The highly nonlinear character of the friction force is obvious, as the damper switches from the stick state to the slip state twice over a period of motion. The Fourier harmonics of the friction force corresponding to this time history are presented in Fig. 7. They show that, although the fundamental harmonic is dominant, neglecting the other harmonics would lead to a significant loss of accuracy.

Finally, the correspondence between the temporal harmonics of the force applied to the reference sector and the spatial harmonics exhibited by the response of the complete structure shows that only 9 spatial modes of vibration are present.

Since the cyclic symmetry theory allows one to deduce the dynamics of the structure from the study of the response of the 3-DOF reference sector, the CPU time associated with solving the nonlinear set of equations of motion is extremely small. In this example, at 200 rad.s^{-1}, this CPU time is 0.04s. This must be compared with the CPU time required to study the response of the complete structure without using its property of cyclic symmetry: in this case, the solution at the same frequency is obtained in 65s.

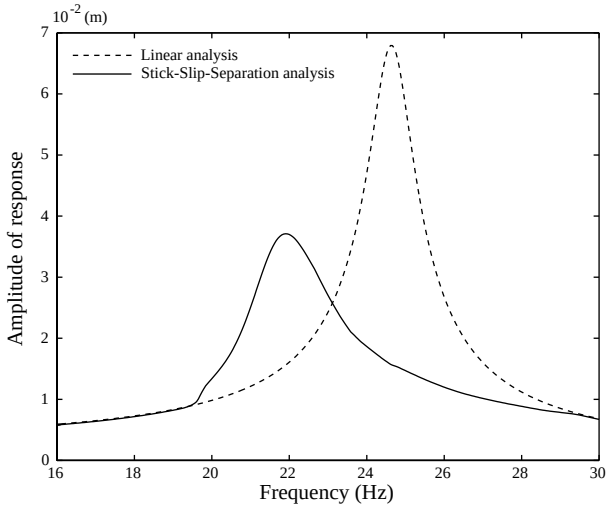

Fig. 9: Linear and nonlinear forced responses of the cantilevered beam presented in Fig. 8.

5.3 Beam subject to friction with variable normal load

The third example studied is depicted in Fig. 8. It consists of a cantilevered beam excited at its tip by a harmonic force of amplitude 100 N in the X direction. The platform of the beam is subject to the action of a friction damper. The dimensions and the mechanical properties of the beam are also described in Fig. 8.

The model of friction damper considered allows for both tangential (along the X direction) and normal (along the Z direction) motion. It is characterized by its tangential stiffness k_t and its normal stiffness k_n. In this example, $k_t = k_n = 2 \times 10^7$ N.m^{-1}. The flexibility of the damper in the Z direction implies that any normal motion of the platform produces a variation of the normal load applied by the damper to the platform. Also, when the displacement of the platform is zero in the Z direction, the normal contact force exerted by the damper on the platform is chosen to be equal to 2000 N.

The beam is condensed out using the Craig-Bampton component mode synthesis. The reduced-order model obtained is made of (1) the X and Z DOFs associated to the node of the tip where the blade is excited, (2) the X and Z DOFs associated to the friction point, and (3), 15 modal coordinates corresponding to the normal modes of vibration of the blade when the physical DOFs mentioned above are fixed.

For this system, the nonlinear analysis is carried out with the harmonics 0, 1, 2, ..., 11, corresponding to a converged solution.

Two forced responses observed at the tip of the blade are described in Fig. 9. The first one corresponds to the mono-harmonic, linear case where the friction damper is

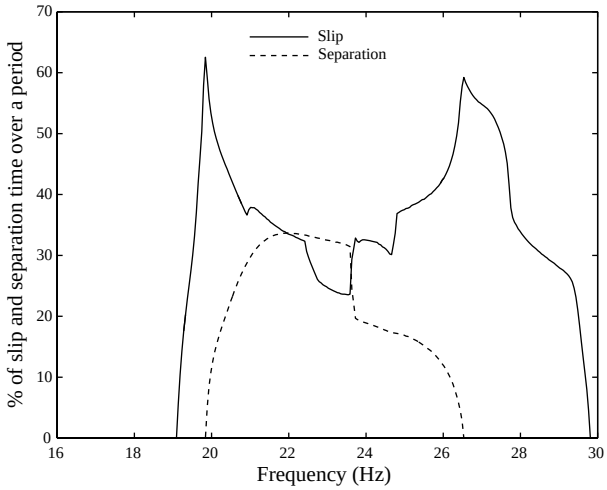

Fig. 10: Percentage of slip time and separation time over a period of motion of the platform.

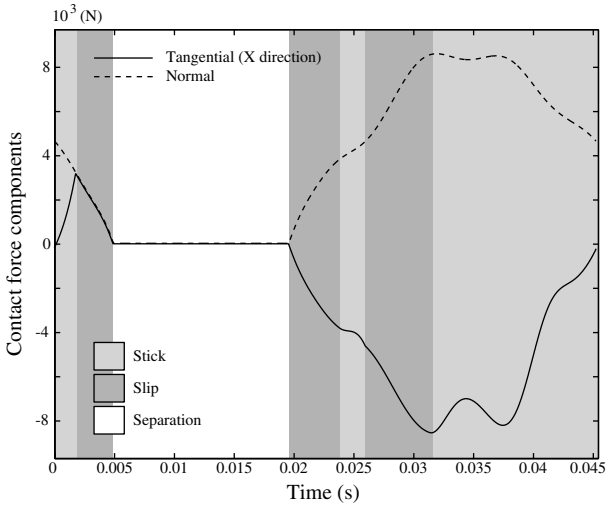

Fig. 11: Time histories of the tangential and normal components of the contact force at 22 Hz.

always attached to the platform, that is, its action on the blade is analog to the effect of an additional stiffness.

The second forced response corresponds to the nonlinear case where the damper can alternate stick, slip and separation phases over a period of motion. It coincides with the linear response for the lowest amplitudes of motions, since the tangential motion of the platform at these low response levels is not large enough to make the damper slip.

As shown in Fig. 10, there exists a large range of frequencies for which the behavior of the damper is highly nonlinear. Near the resonant peak of the nonlinear response, around 22 Hz, the damper spends 30% of the period of motion in the slip state, and also 30% of the period in the separation state where it is no longer in contact with the platform. This is further illustrated in Fig. 11 where the time histories of the tangential and normal contact forces, calculated at 22 Hz, show the complexity of the interaction between the damper and the platform.

Despite the strong nonlinearity exhibited by the system, the hybrid frequency/time domain method is able to calculate the solution of the nonlinear system over the selected range of frequencies without being hindered by convergence problems. The combination of the HFT method and the hybrid Powell algorithm seems therefore effectively adapted to the study of the dynamics of systems featuring complex nonlinear contact forces.

6. CONCLUSION

Two extensions of the Harmonic Balance Method have been proposed in this paper:

The first one is a new method of reduction of the equations of motion to the nonlinear DOFs of systems with friction dampers. It allows the study of structures represented by reduced-order models of relatively large size. These reduced-order models feature a high number of normal modes of vibration and a large number of physical DOFs. Therefore, they offer a better approximation of the dynamics of the structure, and they are of greater interest for parametric studies aimed at optimizing the characteristics and configurations of the dampers. When frequency responses are computed, the computational cost of the new reduction method becomes negligible compared to that of solving the reduced nonlinear system.

The second extension is an exact derivation of the equations of motion for flexible, cyclic structures subject to linear excitations and nonlinear, displacement-dependent forces. Unlike the approximations encountered in the previous literature, it allows one to take into account the elastic coupling existing between the sectors of the structure. A special relation between the temporal harmonics of the excitation and the spatial harmonics of the response of the structure is exhibited.

These two developments are combined with the Hybrid Frequency/Time domain method to study the dynamics of friction damped systems. A modified version of the hybrid Powell algorithm is used to solve the set of nonlinear equations. The numerical examples show that complex, large systems can be efficiently and accurately studied, and they suggest that the method is directly ap-

plicable to the more realistic structures found in the turbomachinery industry.

ACKNOWLEDGEMENTS

This study was carried out for the Société Nationale d'Étude et de Construction de Moteurs d'Aviation. The authors gratefully acknowledge SNECMA for its support.

REFERENCES

[1] Nayfeh, A. and Mook, D., *Nonlinear Oscillations*, John Wiley & Sons, 1979.

[2] Dowell, E. and Schwartz, H., "Forced Response of a Cantilever Beam with a Dry Friction Damper Attached, Part I: Theory," *Journal of Sound and Vibration*, Vol. 91, No. 2, 1983, pp. 255–267.

[3] Ferri, A. and Dowell, E., "The Behavior of a Linear, Damped Modal System with a Non-Linear Spring-Mass-Dry Friction Damper Attached, Part II," *Journal of Sound and Vibration*, Vol. 101, No. 1, 1985, pp. 55–74.

[4] Ferri, A. and Bindemann, A., "Damping and Vibration of Beams with Various Types of Frictional Support Conditions," *Journal of Vibration and Acoustics*, Vol. 114, 1992, pp. 289–296.

[5] Whiteman, W. and Ferri, A., "Displacement-Dependent Dry Friction Damping of a Beam-Like Structure," *Journal of Sound and Vibration*, Vol. 198, No. 3, 1996, pp. 313–329.

[6] Griffin, J., "Friction Damping of Resonant Stress in Gas Turbine Engine Airfoils," *Journal of Engineering for Power*, Vol. 102, 1980, pp. 329–333.

[7] Srinivasan, A. and Cutts, D., "Dry Friction Damping Mechanisms in Engine Blades," *Journal of Engineering for Gas Turbines and Power*, Vol. 105, 1983, pp. 525–530.

[8] Sinha, A. and Griffin, J., "Effects of Friction Dampers on Aerodynamically Unstable Rotor Stages," *AIAA Journal*, Vol. 23, 1985, pp. 262–270.

[9] Sanliturk, K., Imregun, M., and Ewins, D., "Harmonic Balance Vibration Analysis of Turbine Blades with Friction Dampers," *Journal of Vibration and Acoustics*, Vol. 119, 1997, pp. 96–103.

[10] Menq, C., Bielak, J., and Griffin, J., "The Influence of Microslip on Vibratory Response, Part I: A New Microslip Model," *Journal of Sound and Vibration*, Vol. 107, 1986, pp. 279–293.

[11] Menq, C., Griffin, J., and Bielak, J., "The Influence of a Variable Normal Load on the Forced Vibration of a Frictionally Damped Structure," *Journal of Engineering for Gas Turbines and Power*, Vol. 108, 1986, pp. 300–305.

[12] Griffin, J. and Menq, C., "Friction Damping of Circular Motion and Its Implications to Vibration Control," *Journal of Vibration and Acoustics*, Vol. 113, 1991, pp. 225–229.

[13] Sanliturk, K. and Ewins, D., "Modelling Two-Dimensional Friction Contact and its Application Using Harmonic Balance Method," *Journal of Sound and Vibration*, Vol. 193, No. 2, 1996, pp. 511–523.

[14] Menq, C. and Yang, B., "Non-Linear Spring Resistance and Friction Damping of Frictional Constraint Having Two-Dimensional Motion," *Journal of Sound and Vibration*, Vol. 217, No. 1, 1998, pp. 127–143.

[15] Yang, B., Chu, M., and Menq, C., "Stick-Slip-Separation Analysis and Non-Linear Stiffness and Damping Characterization of Friction Contacts Having Variable Normal Load," *Journal of Sound and Vibration*, Vol. 210, No. 4, 1998, pp. 461–481.

[16] Lau, S., Cheung, Y., and Wu, S., "Incremental Harmonic Balance Method with Multiple Time Scales for Aperiodic Vibration of Nonlinear Systems," *Journal of Applied Mechanics*, Vol. 50, 1983, pp. 871–876.

[17] Ferri, A., "On the Equivalence of the Incremental Harmonic Balance Method and the Harmonic Balance-Newton Raphson Method," *Journal of Applied Mechanics*, Vol. 53, 1986, pp. 455–457.

[18] Pierre, C., Ferri, A., and Dowell, E., "Multi-Harmonic Analysis of Dry Friction Damped Systems Using an Incremental Harmonic Balance Method," *Journal of Applied Mechanics*, Vol. 52, No. 4, 1985, pp. 958–964.

[19] Cameron, T. and Griffin, J., "An Alternating Frequency/Time Domain Method for Calculating the Steady-State Response of Nonlinear Dynamic Systems," *Journal of Applied Mechanics*, Vol. 56, 1989, pp. 149–154.

[20] Guillen, J. and Pierre, C., "An Efficient, Hybrid, Frequency-Time Domain Method for the Dynamics of Large-Scale Dry-Friction Damped Structural

Systems," *IUTAM Symposium on Unilateral Multibody Contacts*, edited by F. Pfeiffer and C. Glocker, Kluwer Academic Publishers, Dordrecht, Netherlands, 1999.

[21] Guillen, J., Lagrange, T., and Pierre, C., "An Advanced Damper Model for the Dynamics of Dry Friction Damped Systems," *Proceedings of the 17th Biennial Conference on Mechanical Vibration and Noise, ASME paper DETC99/VIB-8083*, Las Vegas, Nevada, September 1999.

[22] Chen, J. and Menq, C., "Periodic Response of Blades Having Three-Dimensional Nonlinear Shroud Constraints," *Journal of Engineering for Gas Turbines and Power*, Vol. 123, 2001, pp. 901–909.

[23] Nacivet, S., Pierre, C., Thouverez, F., and Jézéquel, L., "Analysis of Periodic Frictional Contact in Finite Elements Problems," *Proceedings of DTEC'01, 2001 ASME Design Engineering Technical Conferences, paper DETC2001/VIB-21735*, Pittsburgh, Pennsylvania, USA, September 2001.

[24] Nacivet, S., Pierre, C., Thouverez, F., and Jézéquel, L., "A Dynamic Lagrangian Frequency-Time Method for the Vibration of Dry-Friction-Damped Systems," *Journal of Sound and Vibration, in print*, 2003.

[25] Lagrange, T., *A Study of the Dynamics of Friction-Damped Blade Assemblies: Cyclic Symmetry and Structure-Like Dampers*, Master's thesis, The University of Michigan, 1999.

[26] Craig, R. and Bampton, M., "Coupling of Substructures for Dynamic Analysis," *AIAA Journal*, Vol. 8, No. 7, 1968, pp. 1313–1319.

[27] Powell, M., "A Hybrid Method for Nonlinear Equations," *Numerical Methods for Nonlinear Equations*, edited by P. Rabinowitz, Gordon and Breach, London, U.K., 1969.

[28] Garbow, B., Hillstrom, K., and More, J., "User Guide for MINPACK-1," Tech. rep., National Argonne Laboratory, 1980.

[29] Berthillier, M., Dupont, C., Mondal, R., and Barrau, J., "Blades Forced Response Analysis with Friction Dampers," *Transactions of the ASME*, Vol. 120, April 1998, pp. 468–474.

APPENDIX

Definition and properties of $\underline{\mathbf{E}}$ and $\underline{\tilde{\mathbf{E}}}$

The complex Fourier matrix $\underline{\mathbf{E}}$ is defined for a n_s-sector cyclic assembly as:

$$\underline{\mathbf{E}}(p,q) = \frac{1}{\sqrt{n_s}} e^{\frac{2j\pi}{n_s}(p-1)(q-1)}, \quad (p,q) \ \in [1, n_s].$$

Assuming that the number of DOFs of a cyclic sector of the assembly is n, the block version $\underline{\tilde{\mathbf{E}}}$ of the Fourier matrix (referred to as extended Fourier matrix) is given by:

$$\underline{\tilde{\mathbf{E}}} = \underline{\mathbf{E}} \otimes \mathbf{I}_n,$$

where $\mathbf{I}_n$ is the n-by-n identity matrix, and $\otimes$ represents the Kronecker product.

The inverse of $\underline{\tilde{\mathbf{E}}}$ is $\underline{\tilde{\mathbf{E}}}^*$, and $\underline{\mathbf{E}}$ satisfies the following property:

$$\underline{\mathbf{E}}^* \underline{\mathbf{u}}_k^{e_o} = \frac{1}{\sqrt{n_s}} \begin{Bmatrix} 0 \\ \vdots \\ 1 \\ \vdots \\ 0 \end{Bmatrix} \leftarrow \begin{array}{l} \text{line } q+1 \text{ such that} \\ q - ke_o \equiv 0 \ [n_s], \end{array}$$

where $\underline{\mathbf{u}}_k^{e_o}$ is defined as:

$$\underline{\mathbf{u}}_k^{e_o} = \left[1, \ldots, e^{(2j\pi p e_o k)/n_s}, \ldots, e^{(2j\pi (n_s-1) e_o k)/n_s}\right]^T.$$

Also, if $\mathbf{A}$ is a $(n \times n_s)$-by-$(n \times n_s)$, real, block-circulant matrix with blocks of size n, then

$$\underline{\tilde{\mathbf{E}}}^* \mathbf{A} \underline{\tilde{\mathbf{E}}} = \mathbf{BDiag}\left[\underline{\mathbf{A}}^0, \ldots, \underline{\mathbf{A}}^{n_s-1}\right],$$

where $\underline{\mathbf{A}}^0, \ldots, \underline{\mathbf{A}}^{n_s-1}$ are n-by-n complex matrices.

Definition and property of the Kronecker product

Given a p-by-q matrix $\mathbf{A}$ and a matrix $\mathbf{B}$, the Kronecker product of A and B is defined as:

$$\mathbf{A} \otimes \mathbf{B} = \begin{bmatrix} \mathbf{A}(1,1)\mathbf{B} & \ldots & \mathbf{A}(1,q)\mathbf{B} \\ \vdots & & \vdots \\ \mathbf{A}(p,1)\mathbf{B} & \ldots & \mathbf{A}(p,q)\mathbf{B} \end{bmatrix}$$

It also satisfies the following property:

$$(\mathbf{A} \otimes \mathbf{B})(\mathbf{C} \otimes \mathbf{D}) = (\mathbf{AC}) \otimes (\mathbf{BD})$$